Available online at www.sciencedirect.com
SCIENCE DIRECT®
Applied Surface Science 236 (2004) 50–56
applied surface science
www.elsevier.com/locate/apsusc

Deposition of yttrium-based thin films on TA6V alloy substrates

R. Siab, G. Bonnet*, J.M. Brossard, J.F. Dinhut

Laboratoire d'Etudes des Matériaux en Milieux Agressifs (LEMMA), Pôle Sciences et Technologie, Université de La Rochelle, Bâtiment Marie Curie, 25 rue Enrico Fermi, 17000 La Rochelle, France

Received 10 February 2004; received in revised form 22 March 2004; accepted 23 March 2004

Available online 21 July 2004

Abstract

Cathodic electrodeposition of yttrium containing thin films was realised on TA6V substrates from a $Y(NO_3)_3$ solution. Experimental conditions to obtain homogeneous and crack free thin films were determined. Subsequent thermal treatment led to an Y_2O_3 coating, expected to provide an increase of TA6V oxidation resistance at high temperatures. The steps occurring during the thermal treatment leading to Y_2O_3 were also investigated.

Keywords: Titanium alloy; Yttrium oxide; Electrodeposition; Coatings

1. Introduction

In the last 10 years, titanium aluminides have received considerable interest, specially in the field of aerospace applications, because of their good mechanical properties and low densities, around 4×10^3 kg m^{-3}. However, the working temperatures of these titanium aluminides are often high and will have to be increased for better yields. It is then necessary to improve their resistance to high temperature oxidation and attempts have been made by introducing alloying elements in the bulk, or through ion implantation or surface coatings. Different elements, such as Mo, W, Nb, or Si have been tested with relative successes concerning high temperature efficiency, some of them leading to a decrease of mechanical properties [1–5].

Otherwise, so-called reactive elements, like hafnium, yttrium and lanthanides, are well known for their beneficial effects on high temperature oxidation behaviour of chromia- or alumina-forming alloys [6,7] and very recently, Wu et al. [8] and Taniguchi et al. [9] have studied, in the case of TiAl intermetallics, the effect on high temperature oxidation resistance of bulk additions of yttrium and hafnium, respectively.

These reactive elements can also be introduced at the alloy surface and electrodeposition of rare earth elements (yttrium, lanthanum, cerium, etc.) over metallic substrates, from aqueous or non-aqueous solutions has recently been reported by different authors [10–12]. Indeed, this technique has received particular attention because it is low cost and permits to obtain homogeneous thin films, with a good control of their thickness, even on complex shaped samples.

In this work, thin yttrium containing films were electrodeposited over TA6V coupons from $Y(NO_3)_3$ water 50 vol.% ethyl alcohol solutions, using a classical three electrode experimental set-up. The deposits were then submitted to a thermal treatment under

* Corresponding author. Tel.: +33-546-458263; fax: +33-546-458229.
E-mail address: gbonnet@univ-lr.fr (G. Bonnet).

0169-4332/$ – see front matter
doi:10.1016/j.apsusc.2004.03.258

argon in order to get an Y_2O_3 coating, the aim being to later study the behaviour of such a coated material under high temperature oxidation conditions.

2. Experimental

In all experiments, TA6V commercial alloy samples (Ti–6Al–4V) were used as substrates. They were cut from a 10 mm diameter rod, with a 2 mm thickness, and drilled to get a 1.5 mm hole. This hole was useful to maintain samples during electrodeposition (the maintaining clip also brought current) and further suspend them (conversion thermal treatment and oxidation testing, in thermobalance). Samples were abraded from 600 SiC paper to 3 μm diamond paste, ultrasonically cleaned in acetone, water and ethyl alcohol and then dried with pulsed warm air before use.

2.1. Experimental set-up for cathodic electrodeposition

The electrochemical bath was a 0.01 M $Y(NO_3)_3$ solution, obtained by dissolving commercial yttrium nitrate ($Y(NO_3)_3$, $6H_2O$, 99.99% purity) in water 50 vol.% ethyl alcohol. Electrodeposition was realised using a classical three electrode experimental set-up, described elsewhere [13,14], including a TA6V sample as cathode, a platinum grid counter electrode and a saturated calomel electrode (SCE) as reference. Deposition experiments were carried out in galvanostatic mode, current density varying from $j = -1$ to -0.05 mA cm^{-2}, at ambient temperature and without stirring. Deposition time was varied from 100 to 7200 s. The variation of the potential versus time was recorded during deposition. After electrodeposition, samples were rinsed with ethyl alcohol and air dried for at least a night before further use or analysis. These experimental conditions were chosen from previous work [14] and were expected to provide uniform and homogeneous thin films with a thickness in the range 50–500 nm.

2.2. Thermal treatment for deposit conversion into Y_2O_3

Coated TA6V substrates (deposit realised at $j = -0.2$ mA cm^{-2} for 1800 s) were introduced in a thermobalance (SETARAM ATG92) and temperature was risen from ambient to 600 °C at a 10 °C min^{-1}, under an inert argon gas atmosphere. Samples were maintained at this temperature for 1 h, then cooled down to room temperature at a 10 °C min^{-1}.

2.3. Deposited and thermally treated films characterisation

Different analytical techniques have been used to characterise the deposited film and its behaviour during conversion thermal treatment. Deposit morphology was observed by optical microscopy, scanning and transmission electron microscopies (SEM, TEM) and atomic force microscopy (AFM). For transmission electron microscopy (TEM) analysis, a deposit formed at $j = -0.2$ mA cm^{-2} during 7200 s was scratched off from the substrate surface and ultrasonically dispersed in ethanol. The obtained particles were collected on a copper grid to be observed. Such a scratched off deposit was also used for differential scanning calorimetry (DSC 2010/2920 cell, TA instruments-universal analysis 2000): it was placed in an aluminum nacelle and heated from 40 to 560 °C at 10 °C min^{-1}, then cooled down to room temperature and finally submitted to a second thermal cycle. Crystallographic structures were determined by X-ray diffraction (XRD), using Co Kα radiation ($\lambda = 0.178897$ nm) at a glancing incidence of 2.5°.

The quantity of deposited yttrium versus deposition time has been determined using inductively coupled plasma-optical emission spectroscopy (ICP-OES). Deposits formed at $j = -0.2$ mA cm^{-2} for 100–7200 s duration were dissolved in a water 5 vol.% nitric acid solution and the obtained solutions were analysed following the usual procedure for this technique.

3. Results and discussion

3.1. Electrodeposition

The electrodeposition, following the described experimental process, leads to the formation of a deposit at the TA6V substrate surfaces, even at very low current densities. Two steps have to be distinguished [15–18]. The first one corresponds to the

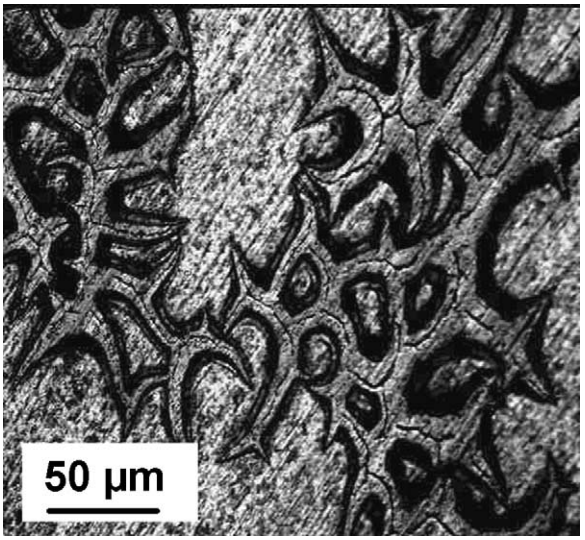

Fig. 1. Optical micrograph of yttrium containing deposit ($j = -1$ mA cm^{-2}, deposition time 1800 s), showing the cracking of the film.

cathodic generation of hydroxyl ions, OH^-, by reduction of O_2, H_2O or NO_3^-, etc.

$$O_2 + 2H_2O + 4e^- \rightleftarrows 4OH^- \quad (1)$$

$$2H_2O + 2e^- \rightleftarrows H_2(g) + 2OH^- \quad (2)$$

$$NO_3^- + H_2O + 2e^- \rightleftarrows NO_2^- + 2OH^- \quad (3)$$

The second should be the precipitation reaction of yttrium hydroxide:

$$Y^{3+}(aq.) + 3OH^-(aq.) \rightleftarrows Y(OH)_3(s) \quad (4)$$

The electrodeposition is done without stirring so that the pH increase and precipitation appear localised close to the substrate surfaces (cathode), leading to the film formation.

The effect of current density on film morphology has been investigated in order to obtain homogeneous and crack free thin films. For a current density of -1 mA cm^{-2}, the film formation is rapid and very important cracks can be observed at the optical microscope (see Fig. 1). To avoid the occurrence of cracking, smaller intensity values, ranging from -0.05 to -0.2 mA cm^{-2} were then retained in order to lower the electrodeposition rate. Fig. 2(a) gives the variation of potential versus time during deposition, at $j = -0.05$, -0.1 and -0.2 mA cm^{-2}. In every case, a very quick decrease of potential is observed in the

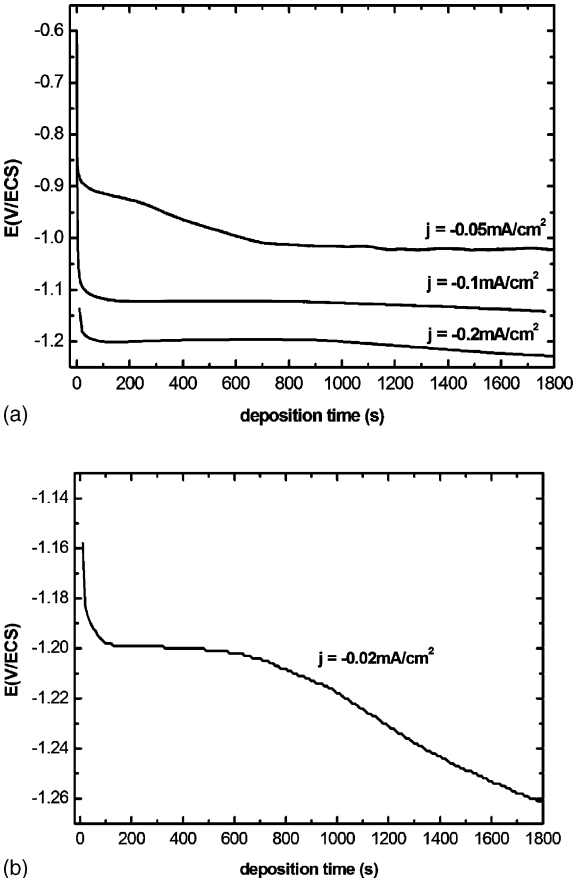

Fig. 2. (a) Variation of potential vs. time during cathodic deposition at $j = -0.05$, -0.1 and -0.2 mA cm^{-2}; (b) magnification of curve obtained at $j = -0.2$ mA cm^{-2}.

first few seconds, corresponding to current stabilisation, then a transition period and, finally, a regular decrease of potential as film thickens (see Fig. 2(b), corresponding to $j = -0.2$ mA cm^{-2} current density, as an example). A very homogeneous and well adherent film is obtained after a 1800 s deposition time under -0.2 mA cm^{-2} and this current density has been chosen for further characterisation.

3.2. Electrodeposited yttrium quantity

The quantity of deposited yttrium versus deposition time, at -0.2 mA cm^{-2} current density, has been determined using ICP-OES. A linear variation of yttrium quantity with time, at least after the first 500 s when film thickens, can be observed on Fig. 3. The deposited

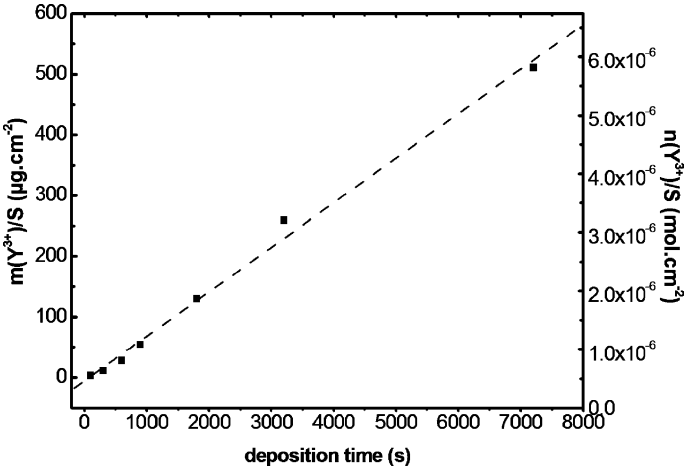

Fig. 3. ICP-OES measurements of the deposited yttrium amounts vs. time (current density $j = -0.2$ mA cm^{-2}).

yttrium quantity appears proportional to the quantity of electricity used, as indicated by the Faraday law. This variation provides an easy control of the film thickness, for the fixed conditions. Moreover, these results are close to those obtained by Brossard et al. on NiCr alloys [14] and suggest that mechanism and deposition rate are independent of metallic substrate nature.

3.3. Deposit characterisation

SEM observation points out that the film formed at $j = -0.2$ mA cm^{-2} for 1800 s covers the whole sample surface and presents a very homogeneous and smooth surface morphology (Fig. 4). AFM microscopy was then used to better characterise the surface. The film is indeed constituted of agglomerated crystallites of nanometer size (Fig. 5). The average roughness determined for a 30 μm × 30 μm surface area is equal to 0.04 μm. The XRD analysis of the deposited film (Fig. 6) gives two broad peaks, showing that the film is not totally amorphous but at least partially crystallised. These peaks located at $2\theta = 11.3^\circ$ and 22.6° do not fit satisfactorily with any yttrium hydroxide JCPDS data file. They can only correspond to the yttrium nitrate hydroxide hydrate: $Y_2(OH)_{6-x}(NO_3)_x{\cdot}0.99H_2O$ (JCPDS data file 32-1435,

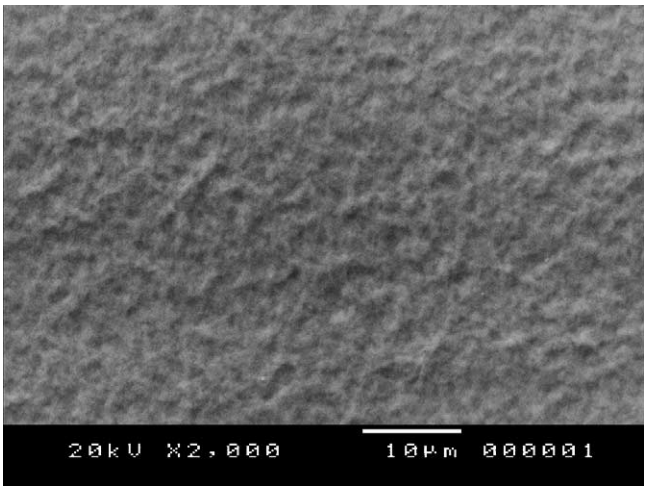

Fig. 4. SEM of electrodeposited coating on TA6V substrate at $j = -0.2$ mA cm^{-2} for 1800 s.

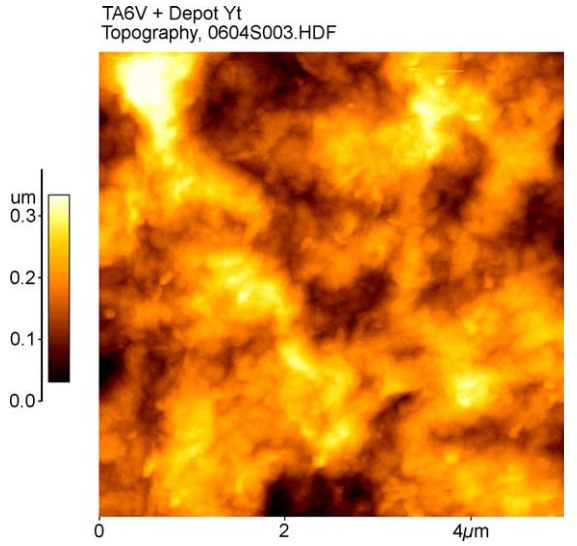

Fig. 5. AFM observation of electrodeposited coating on TA6V substrate at $j = -0.2$ mA cm^{-2} for 1800 s.

$x = 0.86$), identified in the work of Holcombe on yttria hydroxy-salt binders [19].

A deposit was then realised at $j = -0.2$ mA cm^{-2} for 7200 s and scratched off for TEM analysis. A grain could be observed (Fig. 7(a)), the corresponding microdiffraction picture being given in Fig. 7(b). These results are consistent with a crystallised structure and their analysis is in progress.

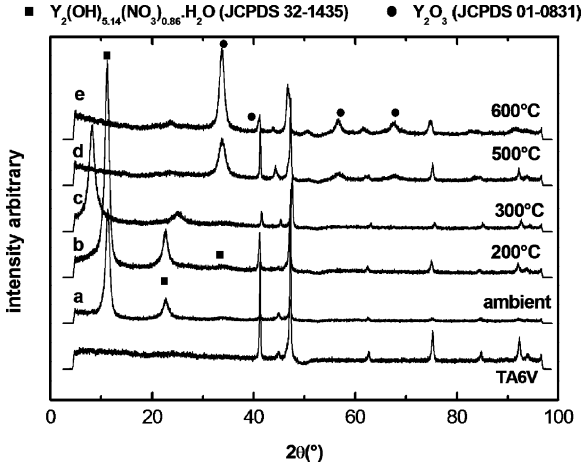

Fig. 6. X-ray diffraction results for uncoated TA6V substrate and coated TA6V samples, without heat treatment (a) and after heat treatment at (b) 200 °C, (c) 300 °C, (d) 500 °C and (e) 600 °C.

3.4. Differential scanning calorimetry (DSC)

DSC measurements on electrodeposited coating have been performed varying temperature from 40 to 560 °C (apparatus limitation). The DSC curve (Fig. 8) exhibits three important endothermic peaks around 130, 320 and 530 °C, attributed to different steps of deposit decomposition. When a second thermal cycle is realised on the same sample, after return to room temperature, no peak can be detected, meaning that the product formed at the end of the first cycle is stable.

The following sequence has been proposed by Holcombe in the case of the decomposition of $Y_2(OH)_{6-x}(NO_3)_x{\cdot}0.99H_2O$, with $x = 0.86$, studied by differential thermal analysis (DTA) [19]:

$$Y_2(OH)_{5.14}(NO_3)_{0.86}0.99H_2O \overset{85-200\,^{\circ}C}{\rightarrow} Y_2(OH)_{5.14}(NO_3)_{0.86} + 0.99H_2O \quad (5)$$

$$Y_2(OH)_{5.14}(NO_3)_{0.86} \overset{230\,^{\circ}C}{\rightarrow} Y_2O_2(OH)_{1.14}(NO_3)_{0.86} + 2H_2O \quad (6)$$

$$Y_2O_2(OH)_{1.14}(NO_3)_{0.86} \overset{520\,^{\circ}C}{\rightarrow} Y_2O_3 + 0.57H_2O + N{-}O \text{ gaseous species} \quad (7)$$

In order to check the sequence in our case, different coated samples, all made under -0.2 mA cm^{-2} for 1800 s, were heated at 200, 300, 500 and 600 °C, respectively, and then analysed by XRD. The corresponding diffractograms are given Fig. 6, together with those of TA6V substrate and untreated coated sample.

At room temperature and at 200 °C, the same two peaks, at $2\theta = 11.3^{\circ}$ and 22.6°, are observed. The endothermic peak at 130 °C was then attributed to the departure of the associated water molecule. After heating at 500 °C, these two peaks have disappeared and new very broad peaks can be seen at $2\theta = 33.8^{\circ}$, 57° and 68°, attributed to Y_2O_3 cubic phase (JCPDS data file 01-0831). After heating at 600 °C, these peaks are still present but sharper and it can be supposed that this is the result of a grain growth process and maybe, the disappearance of possible internal stresses. At intermediate temperature (300 °C), two peaks are again observed but at $2\theta = 8.2^{\circ}$ and 25.1°. These peaks correspond neither at $Y_2(OH)_{5.14}(NO_3)_{0.86}$ nor at Y_2O_3. This phase

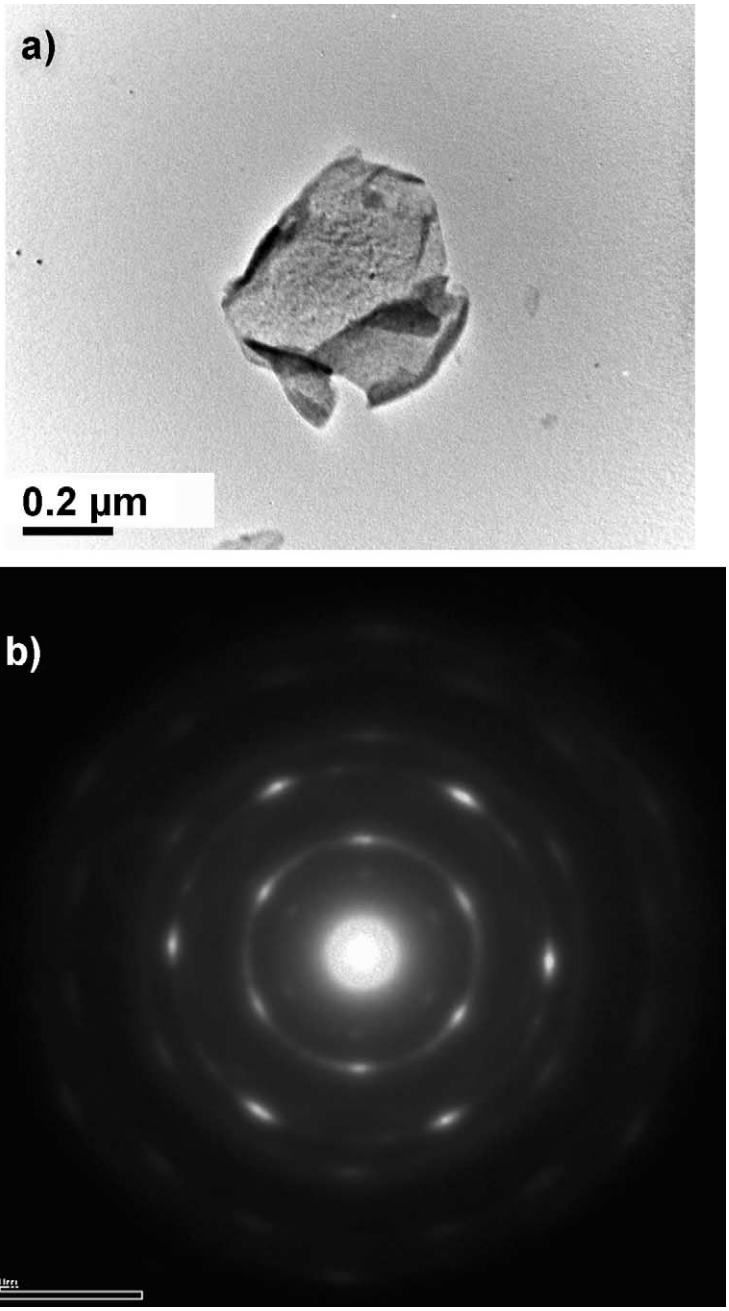

Fig. 7. TEM micrograph of a scratched off grain (a) and selected-area diffraction pattern (b).

appears transitory and could be close to the one proposed by Holcombe [19], i.e. $Y_2O_2(OH)_{1.14}(NO_3)_{0.86}$, resulting from a double dehydration of $Y_2(OH)_{5.14}(NO_3)_{0.86}$ (in agreement with the second DSC peak at 320 °C). This transitory phase effectively leads to Y_2O_3, possibly by a new dehydration and decomposition of nitrate ion into nitrogen oxides (third DSC peak at 530 °C). This transitory phase

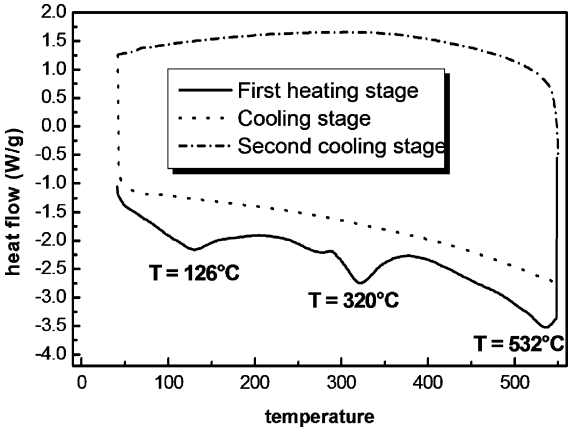

Fig. 8. DSC analysis of scratched off deposit from 40 to 560 °C at 10 °C min^{-1}.

needs to be better identified and this work is currently in progress.

4. Conclusions

Cathodic electrodeposition allowed to achieve an yttrium containing deposit over TA6V substrate surfaces, from a mixed water ethanol yttrium nitrate solution. Effect of imposed current density (in the range -1 to -0.05 mA cm^{-2}) and deposition time (100–7200 s) was investigated. With a -0.2 mA cm^{-2} current density, it was possible to form homogeneous films, crack free even after drying. The deposited film thickness linearly increased with deposition time, giving rise to an easy control of film thickness, in the chosen conditions. The deposit was not an yttrium hydroxide, as expected, but identified as a yttrium hydroxynitrate hydrate compound. By heating from room temperature to 600 °C, this deposited compound transformed, in three steps at 130, 320 and 520 °C, into an yttrium oxide coating, suitable for studying its effects on high temperature behaviour of TA6V alloy.

References

[1] Y. Shida, H. Anada, Oxid. Met. 45 (1996) 197.
[2] M.J. Bennett, A.T. Tuson, High Temperature Intermetallics, Royal Society of London, 1991.
[3] S. Becker, A. Rahmel, M. Schorr, M. Schütze, Oxid. Met. 38 (1992) 425.
[4] C.H. Koo, J.W. Evans, K.Y. Song, T.H. Yu, Oxid. Met. 42 (1994) 529.
[5] R.A. Perkins, K.T. Chiang, G.H. Meier, R. Miller, in: T. Grobstein, J. Doychak (Eds.), Oxidation of High Temperature Intermetallics, The Minerals, Metals and Materials Society, Warrendale, 1988, pp. 157–169.
[6] S. Chevalier, G. Bonnet, J.P. Larpin, J.C. Colson, Corros. Sci. 45 (2003) 1661.
[7] J.-M. Brossard, J. Balmain, A.-M. Huntz, G. Bonnet, Mater. Sci. Forum., submitted for publication.
[8] Y. Wu, S.K. Hwang, S.W. Nam, N.J. Kim, Scripta Mater. 48 (2003) 1655.
[9] S. Taniguchi, H. Juso, T. Shibata, Oxid. Met. 49 (1998) 325.
[10] I. Zhitomirsky, A. Petric, J. Mater. Chem. 10 (2000) 1215.
[11] F.B. Li, R.C. Newman, G.E. Thompson, Electrochem. Acta 42 (16) (1997) 2455.
[12] A. Lgamri, A. Guenbour, A. Ben Bachir, S. El Hajjaji, L. Aries, Surf. Coat. Technol. 162 (2003) 154.
[13] I. Zhitomirsky, A. Petric, Mater. Lett. 50 (2001) 189.
[14] J.M. Brossard, G. Bonnet, J. Balmain, J. Creus, Surf. Coat. Technol., in press.
[15] I. Zhitomirsky, Adv. Colloid Interf. Sci. 97 (2002) 279.
[16] L. Gal-Or, I. Silberman, R. Chaim, J. Electrochem. Soc. 138 (1991) 1939.
[17] K.C. Hu, J. Electrochem. Soc. 134 (1987) 52C.
[18] S. Peulon, D. Lincot, J. Electrochem. Soc. 145 (1998) 864.
[19] C.E. Holcombe Jr., J. Am. Ceram. Soc. 61 (1978) 481.